

Development of a Closed-Form Expression for the Input Impedance of Power-Ground Plane Structures

Minjia Xu, Yun Ji, Todd H. Hubing, Thomas P. Van Doren, James L. Drewniak

Electromagnetic Compatibility Laboratory
Department of Electrical & Computer Engineering
University of Missouri-Rolla
Rolla, MO 65409

Abstract: This paper analyzes the fundamental behavior of PCB power bus structures using the modal expansion method. The results are validated by experiments and full-wave numerical modeling. It is shown that the power bus can be modeled as a series $L_e C$ circuit below the first board resonance frequency. C is the interplane capacitance and L_e is an effective inductance contributed by all the cavity modes. The effects of the layer thickness, port location, board size and the feeding wire radius on the value of L_e are discussed in this study. L_e can be estimated from the geometry parameters of the test board. The goal is to obtain a simple model that can be used to analyze the power bus impedance below the first board resonance.

Introduction

High-speed printed circuit power bus design and modeling is a major concern for EMC engineers. It has been observed that direct radiation from the power bus structure is an increasingly common source of radiated EMI in high-speed systems. In order to develop a basic strategy for designing an optimal power bus, it is necessary to have a better understanding of the fundamental properties of power bus structures commonly used in PCB design.

Power distribution in high-density PCB designs is usually achieved by solid power-ground plane pairs. Figure 1 shows a general power bus structure represented by a rectangular double-sided board of length a and width b . The board consists of two solid copper planes separated by a thin layer of dielectric with thickness h . The feeding port of the power bus structure is modeled as a z -oriented current probe with rectangular cross section of size (dx, dy) . The thickness of the dielectric layer and the dimensions of the port are much smaller than a wavelength at the highest frequency under consideration.

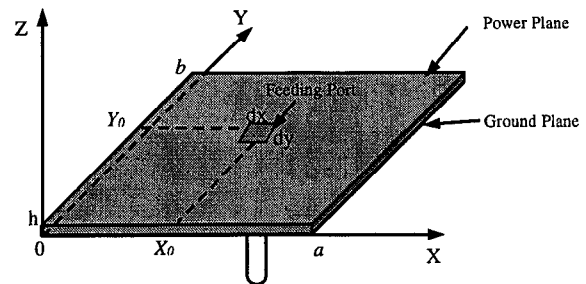


Figure 1. Geometry of the Rectangular Power-Ground Plane Structure

At low frequencies, lumped circuit models can be used to analyze the power-ground plane structure very effectively [1]. At high frequencies where the board dimensions are no longer small compared to a wavelength, 2D or 3D numerical modeling codes are usually required in order to analyze and predict the power bus noise. However, boards with a rectangular or circular shape can be analyzed using a relatively simple and intuitive cavity resonance model.

In this study, a cavity model is used to characterize the input impedance of rectangular power-ground plane structures. The calculation results are validated by experiments and numerical models. The computational error caused by truncating the infinite series is also discussed. Applying the modal expansion method, equivalent circuits based on the cavity model are analyzed. It is shown that below the first board resonance, the power-ground plane structure can be modeled as a $L_e C$ series branch. This model has a series resonance frequency that represents the point where the power-ground plane impedance changes from capacitive to inductive. C is the interplane capacitance of the power bus. The properties of L_e are further examined in this study. A real board example is used to demonstrate the application of the simple power-ground plane model.

Cavity Model of the Rectangular Power-Ground Plane Structure

When the power-ground plane structure is electrically thin, it can be modeled as a TM_z cavity with two perfect electric conductor (PEC) walls representing the power and the ground planes and four perfect magnetic conductor (PMC) sidewalls. The input impedance of this geometry is given by [2,3,4]:

$$Z_{in} = j\omega\mu h \sum_{m=0}^{\infty} \sum_{n=0}^{\infty} \frac{\chi_{mn}^2}{ab(k_{xm}^2 + k_{yn}^2 - k^2)} \times \cos^2(k_{yn}y_i) \cos^2(k_{xm}x_i) \text{sinc}^2\left(\frac{k_{yn}dy_i}{2}\right) \text{sinc}^2\left(\frac{k_{xm}dx_i}{2}\right) \quad (1)$$

where: $k_{xm} = \frac{m\pi}{a}$, $k_{yn} = \frac{n\pi}{b}$, $k = \omega\sqrt{\epsilon\mu}$.

$\chi_{mn}^2 = 1$ for $m=n=0$; $\chi_{mn}^2 = 2$ for $m=0$ or $n=0$; $\chi_{mn}^2 = 4$ for $m \neq 0, n \neq 0$. (x_i, y_i) is the center location of the feeding port. (dx_i, dy_i) is the dimension of the feeding port.

Equation 1 is valid for the input impedance of the lossless power-ground geometry observed from a rectangular feeding port. However, using a perturbation approach, it can be shown that the input impedance with a low-loss dielectric is still very accurately determined by Equation 1 as long as k is replaced by $k_r - jk_i$ [4].

For low loss situations, $k \approx k_r$, and $k_i' = k_r \tan \delta_e$. Here $\tan \delta_e$ is the effective loss tangent representing the total loss that the geometry sustains. When the geometry is fed by coaxial probe, the effective feeding port is represented by a square whose effective cross-section is equal to the area of the circular feeding probe [2].

Experiments and the EMAP5 hybrid FEM/MOM numerical modeling code [5] were used to validate the cavity model. As an example, the input impedance of a 15-cm by 10-cm double-sided board was measured using an HP4291A Impedance Analyzer. The board was fed by a low impedance 85-mil semi-rigid probe at (4cm, 5cm). The radius of the probe's center conductor was 10 mils. The dielectric layer of this board was 55-mil thick with a relative permittivity equal to 4.3. The cutoff frequency of the TM_{10} mode for this geometry was 483MHz. The measurement result had a series resonance at 198 MHz, and a cavity resonance at 488 MHz. The input impedance of this geometry was also calculated using Equation 1 (cavity model) and the EMAP5 numerical

modeling code. For the cavity model, the effective loss tangent was set to 0.01, and the summation was performed up to $N=M=3000$. The results are compared in Figure 2. The input impedance given by the cavity model is consistent with the experimental result and the 3D numerical modeling result up to 1 GHz.

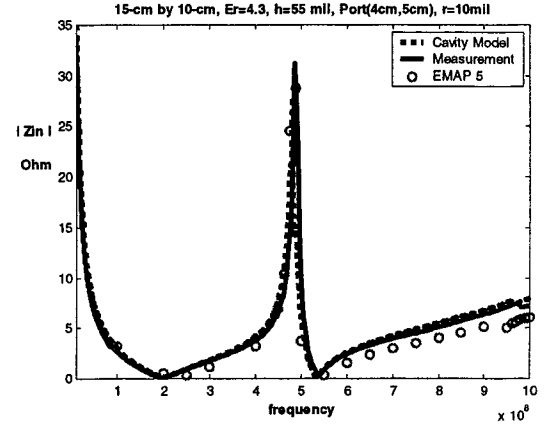


Figure 2. Input Impedance for the 15-cm by 10-cm Board Fed at (4cm, 5cm)

According to the cavity model, the input impedance is the sum of a double infinite series. Each term in the series corresponds to an eigenmode that satisfies the 2D scalar Helmholtz equation and the boundary conditions for the geometry. Based on the modal expansion of Equation 1, the equivalent circuit for the power-ground plane pair is illustrated in Figure 3.

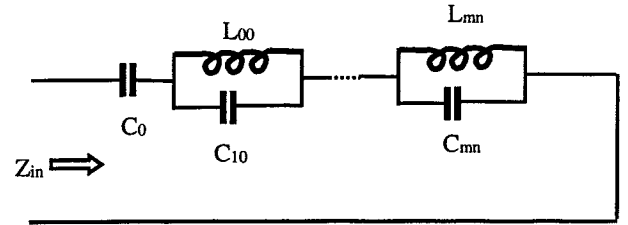


Figure 3. Equivalent Circuit for Lossless Power-Ground Plane Structure

According to the equivalent circuit, the impedance contributed by the TM_{mn} mode is modeled by an LC parallel branch with a resonance frequency equal to the cutoff frequency of this mode. This TM_{mn} mode has an inductive contribution to the input impedance below its cutoff frequency and a capacitive contribution above its cutoff frequency [3]. Therefore, below the cutoff frequency of the TM_{10} mode, the contribution from every mode is inductive. Hence, the power-ground plane

structure can be simply modeled as an L_eC series branch below the TM_{10} cutoff frequency. Here C is the inter-plane capacitance and the effective inductance L_e is given by:

$$L_e = \sum_{m=0}^{\infty} \sum_{\substack{n=0 \\ mn \neq 00}}^{\infty} L_{emn} \quad L_{emn} = \frac{L_{mn}}{1 - \frac{k^2}{k_{xm}^2 + k_{yn}^2}}$$

$$L_{mn} = \mu h \frac{\chi_{mn}^2}{ab} \frac{A^2 B^2}{k_{xm}^2 + k_{yn}^2}$$

$$A = \text{sinc}\left(\frac{k_{yn} dy_i}{2}\right) \text{sinc}\left(\frac{k_{xm} dx_i}{2}\right)$$

$$B = \cos(k_{yn} y_i) \cos(k_{xm} x_i) \quad (2)$$

This infinite series has to be truncated in practical calculations. The eigenmodes in the cavity model are orthogonal to each other, and each cavity resonance peak is solely determined by one specific mode. Therefore, adding or removing terms will not affect the cavity resonance peaks at lower frequencies. This facilitates the quick convergence of the series in the sense of achieving accurate cavity resonances. For the highest frequency of interest, the number of modes that should be included in the calculation can be analytically calculated from:

$$\left(\frac{m\pi}{a}\right)^2 + \left(\frac{n\pi}{b}\right)^2 \leq k^2 \quad (3)$$

For a rough estimation, setting $m_{max} = ak/\pi$, $n_{max} = bk/\pi$ for the highest modes included in the calculation can ensure convergence for cavity resonance frequencies. As an example, for the prior 15-cm by 10-cm board, setting $m_{max} = 11$, and $n_{max} = 7$ can accurately predict all cavity modes below 5 GHz. However, this fast convergence doesn't apply to the series resonance. As discussed before, the first series resonance is caused by the board capacitance and the effective inductance contributed by all cavity modes. Adding more terms will shift the series resonance to a lower frequency. As an example, the input impedance of the 15-cm by 10-cm board was calculated using different numbers of terms. The series and cavity resonance frequencies are listed in Table 1 for the port at (4cm, 5cm). It took many more terms ($m_{max} = n_{max} = 300$) to achieve a 1% error threshold for the series resonance frequency than for the cavity resonance frequency.

Table 1. Convergence of the Series Resonance: 15-cm by 10-cm Board, Port (4cm, 5cm), $r=10$ mils

$n_{max}=m_{max}$	First Series Resonance MHz	First Cavity Resonance MHz
10	268	483
30	233	483
300	191	483
1000	189	483

It was also found that the convergence speed of the series resonance calculation was sensitive to the feeding location and the feeding port dimension, while the convergence speed of the cavity resonance calculation wasn't affected by the feeding port. When the test port was on the corners or edges of the board, it required more terms to achieve convergence of the series resonance calculation. The series and cavity resonance frequencies for Port (0.01cm, 0.01cm) were calculated using the cavity model with a different number of terms, and the results are listed in Table 2. In order to achieve a 5% error threshold for the series resonance frequency, m_{max} and n_{max} had to be set to 3000, which took considerable computation time.

Table 2. Convergence of the Series Resonance: 15-cm by 10-cm Board, Port (0.01cm, 0.01cm), $r=10$ mils

$n_{max}=m_{max}$	First Series Resonance MHz	First Cavity Resonance MHz
10	137	483
30	118	483
300	94	483
1000	87	483
3000	81	483
10000	78	483

Table 3 shows the series and cavity resonance frequencies using different values of n_{max} and m_{max} for the port at (4cm, 5cm). The feeding wire radius, in this case, was 100 mils. The convergence speed of the series resonance calculation was faster than it was with a 10-mil feed probe. Setting m_{max} and n_{max} equal to 30 achieves a 2% error threshold.

Table 3. Convergence of the Series Resonance: 15-cm by 10-cm Board, Port (4cm, 5cm), r=100 mils

$n_{max}=m_{max}$	First Series Resonance MHz	First Cavity Resonance MHz
10	268	483
30	238	483
300	235	483
1000	234	483

Modeling the Power-Ground Plane Structure below the First Cavity Resonance

As revealed by the cavity model, the power-ground plane structure can be simply modeled as a $L_e C$ series branch below the TM_{10} cutoff frequency. The series resonance frequency of this branch is the turning point where the power-ground plane structure changes from capacitive to inductive. In general, the effective inductance, L_e , is a function of frequency. According to Equation 2, the contribution from each eigenmode can be expressed as:

$$L_{emn} = \mu h \frac{\chi_{mn}^2}{ab} \frac{A^2 B^2}{(k_{xm}^2 + k_{yn}^2) - k^2} \quad (4)$$

This term is proportional to the thickness of the dielectric layer. As the result, the effective inductance is also proportional to the thickness of the dielectric layer. However, this relation is only valid when the whole geometry is electrically thin.

The contribution from each mode is related to the feeding port dimension through the two *sinc* functions in factor A . To further investigate the properties of the effective inductance, the input impedances of the 15-cm by 10-cm board with different feed wire radii were calculated. The effective inductance L_e was calculated from the series resonance frequency and plotted in Figure 4. By curve fitting, it was found that the effective inductance is related to the wire radius r by:

$L_e/h = (a + b/\log r)$, where h is the thickness of the dielectric layer. For this example, when the feed wire radii changed from 5 mils to 100 mils, L_e/h dropped from 32.5 pH/mil to 19.5 pH/mil.

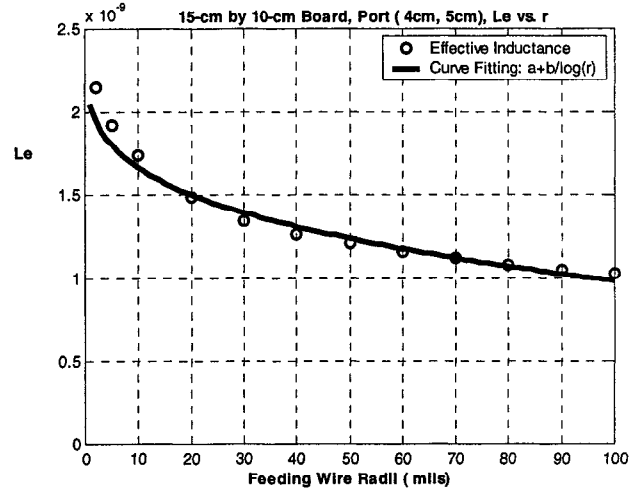


Figure 4. L_e for the 15-cm by 10-cm Board with Different Feeding Wire Radii

The influence of the feeding location on the input impedance and the effective inductance is through the *cosine* function in factor B . The input impedance of a 5-cm by 5-cm square board was calculated for different port locations. The dielectric layer between two solid planes was 40-mil thick, with a relative permittivity equal to 4.0. The feeding location was moved from the corner at (0 cm, 0 cm) toward the center (2.5 cm, 2.5 cm) in 0.5-cm steps. The effective inductance L_e was calculated from the series resonance frequency. The results are plotted in Figure 5. If the power-ground plane is fed on the corner or one edge, the original TM cavity model is not accurate since it does not account for the fringing effect. Applying Equation 1 to these locations results in very high input impedance values and very high values of L_e . However, when the feed port is located away from these singular locations, the equivalent inductance is relatively flat. The minimum L_e occurs when the feed port is located at the center of the geometry (X_c, Y_c). L_e slowly increases as the feed port is moved outward. The relative distance between the feed port and (X_c, Y_c) is defined as D / D_{max} , where D is the distance between the feed port and the center point of the geometry, and D_{max} is the maximum value of D . For a rectangular structure, $D_{max} = 0.5\sqrt{a^2 + b^2}$. Taking the minimum L_e as the reference, the percentage increase of L_e is proportional to the square of the relative distance between the feed port and (X_c, Y_c). The effect of the feeding location on L_e is plotted in Figure 6.

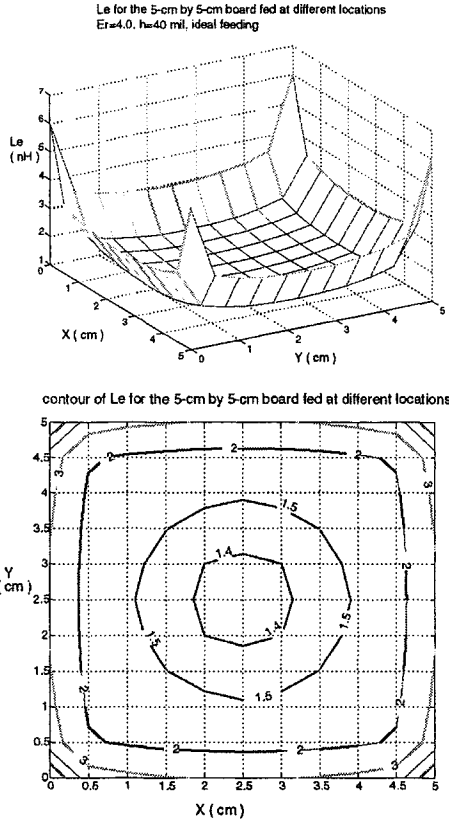


Figure 5. Effective Inductance for the 5-cm by 5-cm Board Fed at Different Locations

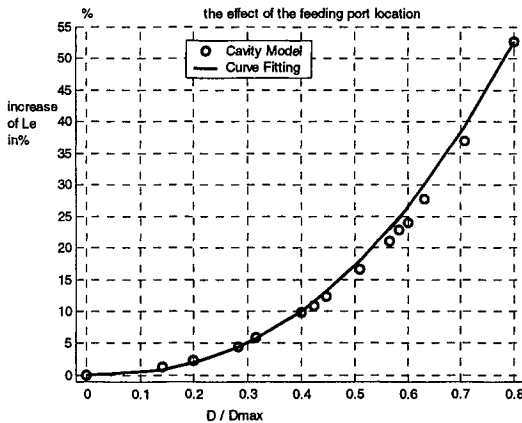


Figure 6. The Effect of Feeding Location on L_e

To investigate the effect of the board size, the same procedure was repeated on a 10-cm by 10-cm board. The thickness and the relative permittivity of the dielectric were the same as for the 5-cm by 5-cm board. The feeding location was moved from (0 cm, 0 cm) to (5 cm, 5 cm) in 1.0-cm steps. The calculated equivalent inductance has the same contour as for the 5-cm by 5-cm

example. When the relative distance between the feed port and the geometric center of the plane is equal, the difference between the L_e for these two examples is within 10%. According to Equation 3, the influence of the board size on the input impedance and the effective inductance is through the following factor:

$$L_{emn} \propto \frac{1}{ab} \times \frac{1}{\frac{(m\pi)^2}{a^2} + \frac{(n\pi)^2}{b^2} - k^2} \quad (5)$$

When the aspect ratio of the plane is not too large, there is only a weak correlation between L_{emn} and the board dimensions.

The prior analysis can be used to estimate L_e for power-ground plane structures based on their geometry. As an example, the L_e of a 7.6-cm by 5.1-cm 6-layer test board was estimated. The board was fed by an SMA jack at location (2.8 cm, 2.55 cm). The radius of the mounting via for the center conductor of the SMA jack was 28 mils. The dielectric layer between the power and the reference plane was 19.4-mil thick with a relative permittivity equal to 4.13. The aspect ratio of this test board was close to 1.5. From Figure 4, L_e was equal to 1.35 nH when the 15-cm by 10-cm board was fed at (4cm, 5cm), and the feed wire radius was about 30 mils. Since L_e is proportional to the thickness of the dielectric layer, the estimated L_e for the 19.4-mil dielectric layer would be about 0.48 nH. For the 15-cm by 10-cm example, the relative distance between the feed location (4 cm, 5 cm) and the geometric center of the board was 0.4. For the 7.6-cm by 5.1-cm board, the relative distance between the feed location (2.8 cm, 2.55 cm) and the geometric center of the board was 0.12. Adjusting for the feed location according to Figure 6 and neglecting the effect of board size, the estimated L_e for the test geometry is 0.44 nH. Now, the test board can be simply modeled as a series $L_e C$ branch below its first cutoff frequency. Here the calculated board capacitance is 287 pF. This model can be used to analyze the input impedance behavior of the test board. The modeled result is compared to a power bus input impedance measurement in Figure 7. A 1-nF bulk decoupling capacitor was then mounted near the feeding SMA jack, and the power bus input impedance measurement was repeated. Assuming the ESL of the bulk decoupling capacitor to be 1.5 nH, the test board with decoupling capacitor can be simply modeled by the lumped circuit shown in Figure 8. In this plot, C_B refers to the board capacitance, and C_d refers to the decoupling capacitance. The modeling parameters can be estimated from the geometry and material parameters of the test board.

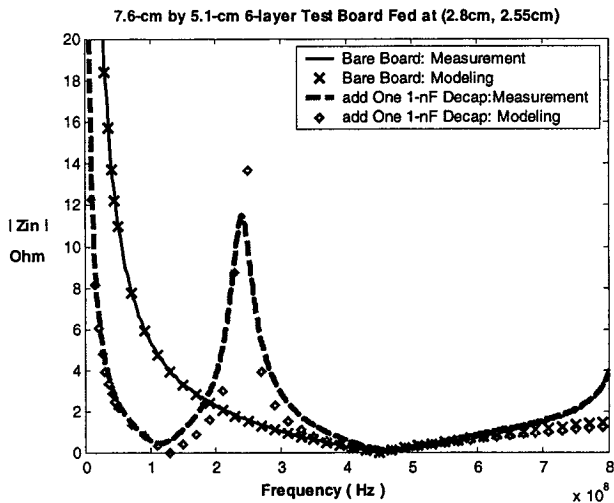


Figure 7. Input Impedance of the 7.6-cm by 5.1-cm 6-Layer Test Board

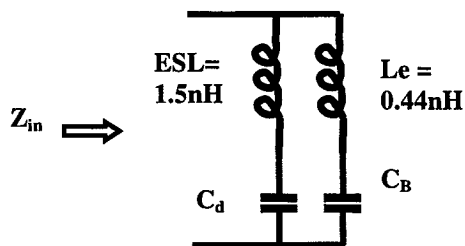


Figure 8. Lumped Circuit Model Below the First Cut-Off Frequency

Conclusions

According to the cavity model, the input impedance of a rectangular power-ground plane structure is the sum of the contributions from all eigenmodes. The input impedance of simple power bus structures at frequencies below the first cavity resonance were calculated using the cavity model and compared to experimental and numerical model results. Truncating the infinite series does not affect the resonance peaks of the input impedance results. However, the series resonance was vulnerable to such truncation. In addition, the convergence speed of the series resonance calculation is much slower than the cavity resonance calculation, and is sensitive to the location and dimension of the feed port.

Applying the modal expansion method, equivalent circuits based on the cavity model were analyzed. It was found that below the first board resonance, the power-ground plane structure can be modeled as an $L_e C$ series branch. Such a model has a series resonance frequency that represents the point where the power-ground plane impedance changes from capacitive to inductive. C is the interplane capacitance of the power bus, and all eigenmodes contribute to the value of L_e .

L_e is proportional to h , the thickness of the dielectric layer. The effects of the feeding location, feed wire radius, and board size on L_e were also discussed. For typical rectangular power-ground plane structures whose aspect ratio is not too large, L_e is around $h \times 30$ pH/mil when the radius of the feed wire is 10 mils. Thicker feed wires result in lower values of L_e . When the power-ground plane is fed at the geometry center, L_e reaches its minimum value. Moving the feeding port outward will increase L_e . According to the cavity model, L_e is singular if the geometry is fed at the corner or edges.

In general, L_e can be estimated from the geometry of the power-ground plane structure. A $L_e C$ series branch can be used to estimate the power bus impedance below the first resonance frequency of the board.

References

- [1] T. H. Hubing, J. L. Drewniak, T. P. Van Doren, and D. M. Hockanson, "Power bus decoupling on multilayer printed circuit boards," *IEEE Transactions on Electromagnetic Compatibility*, vol. 37, No. 2, pp. 155-166, May 1995
- [2] K. R. Carver and J. W. Mink, "Microstrip antenna technology," *IEEE Trans. Antennas and Propagation*, vol. AP-29, No.1, pp. 2-24, Jan. 1981.
- [3] G.-T. Lei, R. W. Techentin, and B. K. Gilbert, "High-frequency characterization of power/ground-plane structures," *IEEE Trans. Microwave Theory and techniques*, vol. 47, No. 5, pp. 562-569, May 1999.
- [4] T. Okoshi, *Planar Circuits for Microwaves and Lightwaves*, Heidelberg, Germany; Springer-Verlag, 1985
- [5] Y. Ji and T. H. Hubing, "EMAP5: A 3D hybrid FEM/MoM code," to appear in *Applied Computational Electromagnetics Society Journal*, Mar. 2000